DE GRUYTER

GRADUATE

Bernhard Blümich,
Sabina Haber-Pohlmeier, Wasif Zia

COMPACT NMR

DE G

Bernhard Blümich, Sabina Haber-Pohlmeier,
Wasif Zia

Compact NMR

DE GRUYTER

Authors
Professor Dr. Bernhard Blümich
RWTH Aachen University
Institut für Technische und
Makromolekulare Chemie (ITMC)
Worringerweg 1
52074 Aachen
bluemich@itmc.rwth-aachen.de

Dr. Sabina Haber-Pohlmeier
RWTH Aachen University
Institut für Technische und
Makromolekulare Chemie (ITMC)
Worringerweg 1
52074 Aachen
haber-pohlmeier@itmc.rwth-aachen.de

Wasif Zia
RWTH Aachen University
Institut für Technische und
Makromolekulare Chemie (ITMC)
Worringerweg 1
52074 Aachen
zia@itmc.rwth-aachen.de

ISBN 978-3-11-026628-3
e-ISBN 978-3-11- 026671-9

Library of Congress Cataloging-in-Publication Data
A CIP catalog record for this book has been applied for at the Library of Congress.

Bibliographic information published by the Deutsche Nationalbibliothek
The Deutsche Nationalbibliothek lists this publication in the Deutsche Nationalbibliografie; detailed bibliographic data are available in the Internet at http://dnb.dnb.de.

Cover image: Measurement of an NMR depth profile of a Roman mosaic in Herculaneum during a study within the Herculaneum Conservation Project, an initiative of the Packard Humanities Institute in collaboration with the Soprintendenza Speciale per i Beni Archeologici di Napoli e Pompei and the British School at Rome.
Typesetting: PTP-Berlin, Protago-TEX-Production GmbH, Berlin
Printing and binding: Hubert & Co. GmbH & Co. KG, Göttingen
♾Printed on acid-free paper
Printed in Germany

www.degruyter.com

Also of Interest

Membrane Systems.
For Bioartificial Organs and Regenerative Medicine
Loredana De Bartolo, Efrem Curcio, Enrico Drioli 2014
ISBN 978-3-11-026798-3, e-ISBN 978-3-11-026801-0

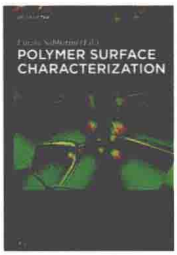

Polymer Surface Characterization
Luigia Sabbatini (Ed.) 2015
ISBN 978-3-11-027508-7, e-ISBN 978-3-11-028811-7

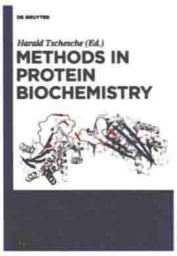

Methods in Protein Biochemistry
Harald Tschesche (Ed.) 2011
ISBN 978-3-11-025233-0, e-ISBN 978-3-11-025236-1

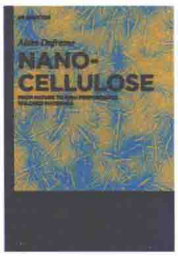

Nanocellulose.
From Nature to High Performance Tailored Materials
Alain Dufresne 2012
ISBN 978-3-11-025456-3, e-ISBN 978-3-11-025460-0

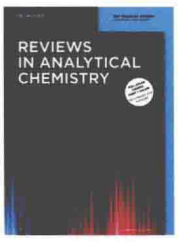

Reviews in Analytical Chemistry
Israel Schechter (Editor-in-Chief)
ISSN 0793-0135, e-ISBN 2191-0189

Foreword

NMR is a complicated business. When we want to learn the trade, being fascinated by all these wonderful experiments the NMR experts tell us are simple to do, we get confronted with mountains of information about pulses, flip angles, the rotating coordinate frame, the density matrix, and more. How is it, that we cannot do NMR in the same manner as we are used to operating a DVD player or some other sophisticated technical gadget like a cell phone. Clearly, an NMR spectrometer is a bit more complicated than a coffee machine, and so the instructions for operating a spectrometer are not expected to be trivial. But is an NMR spectrometer really more complicated than a cell phone? Probably not! Nevertheless we can operate a mobile phone without knowing the technical details about its function and the electronics inside. So why can we not operate an NMR spectrometer and get decent results on a level of expertise similar to that required using a cell phone?

Today one of the most challenging tasks is the miniaturization of NMR machines for use as dedicated and personalized devices. Because the use of such compact devices is comparatively new and these NMR devices become more popular, this book intends to be a guide to their use and applications by providing the basic knowledge and operating instructions to perform successful NMR measurements. The content focuses on compact and mobile NMR machines for the analysis of materials and processes, because this technology is most likely to be in demand by investigators who have little to no knowledge about NMR. Following a basic introduction to NMR and compact NMR equipment in Chapter 1, the experimental set-up is discussed in Chapter 2. Several general types of NMR experiments are described in Chapter 3. Representative applications of these experiments to liquids, polymers, biological tissue, porous media, and objects from cultural heritage are collected in Chapters 4 to 8. For each case, a description of the measurement and data evaluation procedures is given with reference to the principles and procedures explained in the preceding chapters. Each description follows the same pattern including the objective, the theoretical background, the pulse sequences and parameters, beginners-level measurements, advanced-level measurements, and data processing. It is hoped, the information given will help the NMR novice to successfully conduct measurements with compact NMR equipment although it is not quite yet at the level of operating a cell phone.

This book has benefitted from the help of many friends and members of the Aachen NMR research group. They contributed earlier versions of some sections of the book, helped with proof reading, checked the pulse sequences and phase tables, and most importantly provided many of the experimental data given as examples in the text. We thank Alina Adams, Sophia Anferova, Vladimir Anferov, Stephan Appelt, Juliane Arnold, Maria Baias, Peter Blümler, Federico Casanova, Ernesto Danieli, Vasiliki Demas, Dan Demco, Gunnar Eidmann, Ralf Eymael, Stefan Glöggler, Nicolae Goga, Andreas Guthausen, Gisela Guthausen, Agnes Haber, Rolf Haken,

Song-I Han, Christian Hedesiu, Volker Herrmann, Jürgen Kolz, Kidist Hailu, Bharatam Jagadeesh, Martin Klein, Kai Kremer, Rance Kwamen, Maxime Van Landeghem, Dirk Oligschläger, Eva Paciok, Josefina Perlo, Juan Perlo, Pablo Prado, Gabriel Rata Doru, Ralf Savelsberg, Udo Schmitz, Andrea Schweiger, Shatrughan Sharma, Siegfried Stapf, Oscar Sucre, Yadoallah Teimouri, Jochen Vieß, Alexandra Voda, and Anette Wiesmath for their scientific contributions to the contents of this book. Eiichi Fukushima, Tia Ishi, Eva Paciok and Lutz Weihermüller helped with proof reading early versions of the book and demanding chapters. Individual figures were kindly supplied by Gisela Guthausen, Burkhard Luy, Antonio Marchi, Peter McDonald, and Frank Rühli. Special thanks are from Bernhard to Joanie for accepting endless evenings of an absent minded husband, from Sabina to Andreas for many discussions even before breakfast, and from Wasif to his mother Rifqua Ejaz for listening to him everyday and to Aroosa Ijaz for standing by him.

Aachen, 31st August 2013

Bernhard Blümich
Sabina Haber-Pohlmeier
Wasif Zia

List of Symbols

a_{fast}	amplitude of a rapidly decaying signal component
a_{slow}	amplitude of a slowly decaying signal component
a_{ij}	component amplitudes
A	absorption signal, cross sectional area
b	power exponent in the Kohlrausch function
b_1, b_2	diffusion attenuation coefficient
B	magnitude of the magnetic field
$\boldsymbol{B}$	magnetic field vector
B_0	magnitude of the homogeneous magnetic field
B_1	amplitude of the radio-frequency magnetic field
$\boldsymbol{B}_1$	vector of the rf magnetic field
$\boldsymbol{B}_{\text{eff}}$	effective field
$\boldsymbol{B}_{\text{fic}}$	fictive field
B_z	z-component of the magnetic field vector
C	constant
C_1, C_2	constants
C_{M}	spin-density contrast
C_{w}	contrast of the weight parameter, water capacity function
dB	decibel
d_{i}	diameter of the interface domain
d_{m}	diameter of the mobile domain
d_{r}	diameter of the rigid domain
D	diffusion coefficient, dispersion signal, soil water diffusivity
D_0	self-diffusion coefficient of the pure substance
D_{eff}	effective diffusion coefficient
exp	exponential function
E	energy
$E_\uparrow$	energy of spins pointing up
$E_\downarrow$	energy of spins pointing down
f	scaling factor
FT	Fourier transformation
G	magnitude of the magnetic field gradient, shear modulus
$\boldsymbol{G}$	magnetic field gradient vector
G_{eff}	effective field gradient
G_{int}	internal field gradient
G_{max}	maximum gradient value
G_{phase}	phase-encoding gradient
G_{read}	read gradient
G_{slice}	slice-selection gradient
G_x	x-component of the gradient vector
$G_{x,\text{max}}$	maximum gradient in x-direction
h	hydraulic head, Planck's constant
^{1}H	hydrogen nucleus
i	square root of –1
J	water flow velocity
$\boldsymbol{k}$	wave vector
k_{B}	Boltzmann constant
k_{ij}	exchange rate
k_y	wave number in y-direction
$k_{y,\text{max}}$	maximum wave number in y-direction
k_z	wave number in z-direction
$k_{z,\text{max}}$	maximum wave number in z-direction
$\mathbf{K}$	matrix of exchange rates
K	hydraulic conductivity
K_{S}	hydraulic conductivity at full saturation
l_{d}	diffusion length
ln	natural logarithm
log	logarithm of base 10
L	length
L_0	initial length
m_{s}	mass of solid phase
m_{t}	total mass
m_{w}	mass of water phase
$\boldsymbol{M}$	nuclear magnetization vector
M_0	thermodynamic equilibrium magnetization, spin density
$M_{0\text{ref}}$	spin density of a reference compound
M_2	second moment
$M(t)$	complex transverse magnetization
M_{c}	molecular weight between cross-links in an elastomer
M_{n}	number-average molecular weight
M_x	component of the magnetization vector in x-direction
M_y	component of the magnetization vector in y-direction
M_z	component of the magnetization vector in z-direction
n	number, cross-link density, van Genuchten parameter
$n_\uparrow$	number of spins pointing up

$n_\downarrow$	number of spins pointing down
n_1, n_2	numbers
n_{acq}	number of acquired data points
n_E	number of echoes
$n_{f,max}$	maximum number of frequency encoding steps
n_G	number of gradient steps
$n_{p,max}$	maximum number of phase encoding steps
n_s	number of scans
p	Laplace variable
P	probability density
$P(r)$	droplet size distribution
q	fraction
Q	volume flow rate
r	radius, magnitude of space vector
$\boldsymbol{r}$	space vector
$\langle r \rangle$	mean radius
R	ideal gas constant, constant, magnitude of the displacement vector, hydrodynamic radius
$\mathbf{R}$	relaxation matrix
RX	receiver
s	signal
s_{2Q}	double quantum signal
s_d	signal of a distribution
s_{ref}	reference signal
S	spectrum, Fourier transform of s, surface area
SFC	solid fat content
t	time
t_{acq}	acquisition time
t_d	dead time
t_E	echo time, dito t_{E1}, t_{E2}, t_{E2}
$t_{E,eff}$	effective echo time
t_f	filter time
t_m	mixing time
t_{MQ}	multiquantum evolution time
t_p	pulse width
t_{phase}	duration of G_{phase}
t_{read}	duration of G_{read}
t_R	repetition time, recycle delay
t_z	storage time for a longitudinal magnetization
t_0	recovery time
t_1	evolution time, evolution period
t_2	detection time, detection period
t_{90}	duration of the 90° pulse
t_{180}	duration of the 180° pulse
T	absolute temperature
TX	transmitter
T_1	longitudinal relaxation time
$1/T_1$	longitudinal relaxation rate
$1/T_2$	transverse relaxation rate
$1/T_{1bulk}$	longitudinal relaxation rate of the bulk
$1/T_{2bulk}$	transverse relaxation rate of the bulk
$1/T_{2diff}$	transverse relaxation rate for diffusion in gradients
$1/T_{2surf}$	surface transverse relaxation rate
T_0	time constant
T_{1o}	longitudinal relaxation time of the oil phase
T_{1w}	longitudinal relaxation time of the water phase
T_2	transverse relaxation time in homogeneous field
T_2^*	transverse relaxation time including field inhomogeneity
T_{2A}	transverse relaxation time of component A
T_{2B}	T_2 of component B
T_{2C}	T_2 of component C
T_{2bulk}	transverse relaxation time of the bulk
T_{2eff}	effective transverse relaxation time
$T_{2eff,0}$	reference effective transverse relaxation time
$T_{2eff,aniso}$	anisotropic T_{2eff}
$T_{2eff,inter}$	T_{2eff} of the interfacial component
$T_{2eff,iso}$	isotropic T_{2eff}
$T_{2eff,long}$	T_{2eff} of the mobile component
$T_{2eff,short}$	T_{2eff} of the rigid component
T_{2lm}	logarithmic mean value of the relaxation distribution
T_{2long}	long relaxation time
T_{2short}	short relaxation time
u	real part of the NMR signal recorded in the time domain
U	real part of the spectrum
v	imaginary part of the NMR signal recorded in the time domain
V	imaginary part of the spectrum, volume
V_g	volume of gas phase
V_s	volume of solid phase
V_t	total volume
V_w	volume of water phase
w	weight parameter, relaxation-weighted spin density

x, y, z	space coordinates
$\boldsymbol{x}, \boldsymbol{y}, \boldsymbol{z}$	unit vectors along the Cartesian space coordinates
x_A	number fraction of component A, crystallinity
x_B	number fraction of component B
x_C	number fraction of component C
x_i	number fraction of the interfacial component
x_m	number fraction of the mobile component
x_{max}	field of view in x-direction
x_r	number fraction of the rigid component
z_{max}	field of view in z-direction
α	flip angle of an rf pulse, van Genuchten parameter
α_E	Ernst angle
γ	gyromagnetic ratio
Δ	diffusion time
ΔG_{phase}	increment of G_{phase}
ΔG_z	increment of gradient in z-direction
Δt	dwell time, sampling interval
Δt_1	increment of the evolution time
Δt_E	increment of the echo time
$1/\Delta x$	spatial resolution in x-direction
$\Delta\phi$	phase increment
$\Delta\nu_{1/2}$	line width in Hz
$\Delta\omega_{1/2}$	line width in rad/s
δ	chemical shift, duration of a gradient pulse
δ_{max}	maximum chemical shift
ϵ	strain
φ	precession angle
φ_1	transmitter phase of pulse 1
φ_{acq}	receiver phase for data acquisition
φ_{RX}	receiver phase
φ_{TX}	transmitter phase
ϕ	phase error
ϕ_0	constant phase correction parameter
ϕ_1	linear phase correction parameter
Φ	porosity
η	viscosity
κ	fluid permeablity
Λ	elongation ratio
ν	frequency in Hz
ν_0	Larmor or precession frequency in Hz
ν_{max}	maximum frequency
ν_r	reference frequency
ν_{rf}	NMR frequency for transmitter and receiver in Hz
θ_m	water content of mass fraction
θ_r	bound water content
θ_V	volumetric water content
Θ	normalized water saturation
Θ_S	water saturation
ω	frequency in rad/s
ω_0	Larmor frequency in rad/s
ω_1	nutation frequency in rad/s
ω_f	final frequency in rad/s
ω_i	initial frequency in rad/s
ω_{rf}	NMR frequency for transmitter and receiver in rad per second
Ω	frequency offset from the rf transmitter frequency
π	half the circumference of the unit circle
ϖ_D	residual dipole-dipole interaction
θ	polar angle
ρ	density
$\rho_{1,2}$	surface relaxivities
ρ_s	density of solid particles
ρ_t	density of bulk soil
σ	standard deviation
τ	delay between the first and the second pulse in an echo sequence
τ_c	correlation time of molecular motion
τ_{ij}	exchange time between sites i and j
ψ	total water potential
ψ_m	matrix potential
ψ_o	osmotic potential
ψ_p	additional air pressure potential
ψ_z	gravitational potential
ψ_H	hydraulic potential
ψ_Ω	overburden potential

List of Acronyms

1D	one-dimensional
2D	two-dimensional
2Q	double quantum
3D	three-dimensional
ADC	Analog-to-Digital Converter
AOCS	American Oil Chemists' Society
ASCII	Amercian Standard Code for Information Interchange
CLI	Command Line Interface
COSY	COrrelation SpectroscopY
CPMG	Carr, Purcell, Meiboom, Gill
C-S-H	calcium silicate hydrate
CT	Computer Tomography
CUFF	Cut-open, Uniform, Force Free
CYCLOPS	CYClically Ordered Phase Sequence
DOSY	Diffusion Ordered SpectroscopY
EXSY	EXchange SpectroscopY
FID	Free Induction Decay
FLASH	Fast Low Angle Shot
FSP	Fiber Saturation Point
FT	Fourier Transformation
GARfield	Gradient At Right angle to the magnetic field
GPC	Gel Permeation Chromatography
HetCor	Hetero-nuclear Correlation
HDPE	High-Density PolyEthylene
IR	InfraRed
ISO	International Organization for Standardization
LDPE	Low-Density PolyEthylene
LLDPE	Linear Low-Density PolyEthylene
ln	logarithmus naturalis
MAS	Magic Angle Spinning
MIP	Mercury Intrusion Porosimetry
MOUSE	Mobile Universal Surface Explorer
MRI	Magnetic Resonance Imaging
MRT	Magnetic Resonance Tomography
MQ	MultiQuantum
NMR	Nuclear Magnetic Resonance
NOESY	Nuclear Overhauser Effect SpectroscopY
o/w	oil-in-water
PE	PolyEthylene
PFG	Pulsed Field Gradient
Prospa	Processing package
PVC	PolyVinylChloride
PTFE	PolyTetraFluoroEthylene
rf	radio frequency
RARE	Rapid Acquisition with Relaxation Enhancement
RMS	Root Mean Square
ROSY	Relaxation Ordered Spectoscopy
RPA	Rubber Process Analyzer
RX	Receiver
SEC	Size-Exclusion Chromatography
SFC	Solid Fat Content
SNR	Signal-to-Noise Ratio
SPAC	Soil Plant Atmosphere Continuum
S/V	Surface-to-Volume ratio
SQUID	Superconducting Quantum Interference Device
TX	Transmitter
USB	Universal Serial Bus
UV	Ultra Violet
w/c	water/cement ratio
w/o	water-in-oil

Contents

1 Introduction to NMR

The chemist calls it *NMR* and the medical doctor *MRI*. *Nuclear magnetic resonance* (NMR) is the most popular tool in chemistry to analyze molecular structures, and *magnetic resonance imaging* (MRI) is a non-invasive diagnostic tool in the hospital that provides high-contrast *images* of tissues depicting the brain functions and the beating heart. In both cases large and expensive superconducting magnets are employed (Fig. 1.0.1), which magnetize the object by aligning the atomic nuclei inside the magnet. The resulting magnetization can be triggered by radio frequency waves to rotate around the direction of the magnetic field. Depending on the operating mode, the frequency *spectrum* of the rotating nuclear magnetization provides the chemist with molecular information and the medical doctor with anatomical images, while the materials scientist may be interested in the decay of the *impulse response* to learn about physical properties of a solid object like a wet wall.

1.1 NMR: Nuclear Magnetic Resonance

NMR can be defined as a physical phenomenon which is utilized to investigate molecular properties of matter by irradiating atomic nuclei in a *magnetic field* with electromagnetic *radio waves*. Many nuclear isotopes possess an angular momentum called *spin*. In classical terms, spins appear to rotate around an axis like a bicycle wheel (Fig. 1.1.2a). For atomic nuclei, however, the somewhat unusual laws of *quantum mechanics* apply. For example, every spin is associated with a *magnetic moment* like the

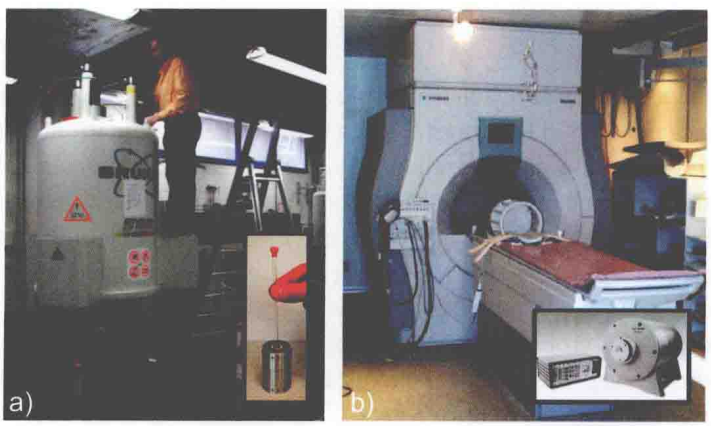

Figure 1.0.1. High-field NMR machines with superconducting magnets and compact, low-field machines with permanent magnets (insets). (a) Magnets for chemical analysis. (b) Magnets for magnetic resonance imaging (MRI). The patient or the object is positioned in the center of the magnet hole. The bulky electronics of medical MRI machines are typically hidden in a separate room.

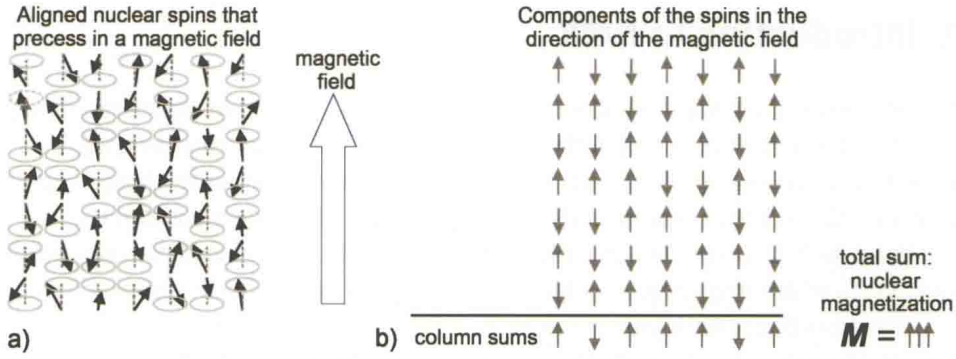

Figure 1.1.1. Schematic drawing of 49 out of 10^{23} proton spins which are aligned in a magnetic field. (a) Each spin appears to rotate or 'precess' around the direction of the magnetic field in a manner similar to a spinning bicycle wheel, which precesses around the direction of the gravitational field (Fig. 1.1.2a). (b) The up and down states of the spins are more easily recognized when only the part of the spin vector parallel to the direction of the magnetic field is drawn. Because each spin is a magnet, each of these arrows represents a magnet. The nuclear magnetization $\boldsymbol{M}$ is the sum of the magnetizations from each component magnet.

needle of a compass. Depending on the magnitude of the spin, it can align with a magnetic field in different stable orientations, which differ in their inclination angles with respect to the magnetic field and therefore also differ in their energies (Fig. 1.1.1a). *Protons*, the most abundant nuclear spins in organic matter, align in two states, called up (↑) and down (↓). The relative numbers $n_\uparrow$ and $n_\downarrow$ of spins for the two states with energies $E_\uparrow$ and $E_\downarrow$ follow the *Boltzmann distribution*, where k_B is the Boltzmann constant and T is the temperature in Kelvin,

$$\frac{n_\downarrow}{n_\uparrow} = \exp\{-(E_\downarrow - E_\uparrow)/(k_B T)\}. \tag{1.1.1}$$

The *nuclear magnetization* $\boldsymbol{M}$ of a macroscopic sample with some 10^{23} spins is formed by the difference $n_\uparrow - n_\downarrow$ of the number of spins with different orientations (Fig. 1.1.1b).

Because the resulting magnetization $\boldsymbol{M}$ is composed of an unimaginably large number of quantum mechanical entities, it behaves like a classical *magnet*, which spins around its magnetization axis. It interacts with a magnetic field $\boldsymbol{B}_0$ in the same way as a *gyroscope* e.g., in the way a spinning bicycle wheel interacts with the gravitational field (Fig. 1.1.2a): When not aligned with the direction of the field, the magnetization axis rotates around the direction of the field (Fig. 1.1.2b). This rotation is called precession. The *precession frequency* or *Larmor frequency* ω_0 is proportional to the strength B_0 of the applied field,

$$\omega_0 = 2\pi\nu_0 = \gamma B_0 \tag{1.1.2}$$

where the *gyromagnetic ratio* γ is a constant specific to the type of atomic nucleus, and $\nu_0 = (E_\downarrow - E_\uparrow)/h$, where h is Planck's constant. For example, the frequency ν_0 for